A LETTERS JOURNAL EXPLORING THE FRONTIERS OF PHYSICS

OFFPRINT

Frequency spectrum of a superconducting metadevice

J. A. Blackburn, M. Cirillo and N. Grønbech-Jensen

EPL, **115** (2016) 50004

Please visit the website
www.epljournal.org

Note that the author(s) has the following rights:
– immediately after publication, to use all or part of the article without revision or modification, **including the EPLA-formatted version**, for personal compilations and use only;
– no sooner than 12 months from the date of first publication, to include the accepted manuscript (all or part), **but not the EPLA-formatted version**, on institute repositories or third-party websites provided a link to the online EPL abstract or EPL homepage is included.
For complete copyright details see: https://authors.epletters.net/documents/copyright.pdf.

A Letters Journal Exploring the Frontiers of Physics

AN INVITATION TO SUBMIT YOUR WORK

epljournal.org

The Editorial Board invites you to submit your letters to EPL

EPL is a leading international journal publishing original, innovative Letters in all areas of physics, ranging from condensed matter topics and interdisciplinary research to astrophysics, geophysics, plasma and fusion sciences, including those with application potential.

The high profile of the journal combined with the excellent scientific quality of the articles ensures that EPL is an essential resource for its worldwide audience. EPL offers authors global visibility and a great opportunity to share their work with others across the whole of the physics community.

Run by active scientists, for scientists

EPL is reviewed by scientists for scientists, to serve and support the international scientific community. The Editorial Board is a team of active research scientists with an expert understanding of the needs of both authors and researchers.

OVER
568,000
full text downloads in 2015

18 DAYS
average accept to online publication in 2015

20,300
citations in 2015

"We greatly appreciate the efficient, professional and rapid processing of our paper by your team."

Cong Lin
Shanghai University

Six good reasons to publish with EPL

We want to work with you to gain recognition for your research through worldwide visibility and high citations. As an EPL author, you will benefit from:

1. **Quality** – The 60+ Co-editors, who are experts in their field, oversee the entire peer-review process, from selection of the referees to making all final acceptance decisions.
2. **Convenience** – Easy to access compilations of recent articles in specific narrow fields available on the website.
3. **Speed of processing** – We aim to provide you with a quick and efficient service; the median time from submission to online publication is under 100 days.
4. **High visibility** – Strong promotion and visibility through material available at over 300 events annually, distributed via e-mail, and targeted mailshot newsletters.
5. **International reach** – Over 3200 institutions have access to EPL, enabling your work to be read by your peers in 100 countries.
6. **Open access** – Articles are offered open access for a one-off author payment; green open access on all others with a 12-month embargo.

Details on preparing, submitting and tracking the progress of your manuscript from submission to acceptance are available on the EPL submission website **epletters.net**.

If you would like further information about our author service or EPL in general, please visit **epljournal.org** or e-mail us at **info@epljournal.org**.

EPL is published in partnership with:

European Physical Society | Società Italiana di Fisica | EDP Sciences | IOP Publishing

A Letters Journal Exploring the Frontiers of Physics

September 2016

EPL, **115** (2016) 50004
doi: 10.1209/0295-5075/115/50004

www.epljournal.org

Invited Research Article

Frequency spectrum of a superconducting metadevice

J. A. Blackburn[1], M. Cirillo[2(a)] and N. Grønbech-Jensen[3,4]

[1] *Physics and Computer Science, Wilfrid Laurier University - Waterloo, Ontario, Canada*
[2] *Dipartimento di Fisica and MINAS-Lab, Università di Roma "Tor Vergata" - 00133 Roma, Italy*
[3] *Department of Mathematics, University of California - Davis, CA 95616, USA*
[4] *Department of Mechanical and Aerospace Engineering, University of California - Davis, CA 95616, USA*

received 23 August 2016; accepted in final form 22 September 2016
published online 13 October 2016

PACS 03.67.Lx – Quantum computation architectures and implementations
PACS 74.50.+r – Tunneling phenomena; Josephson effects
PACS 85.25.Cp – Josephson devices

Abstract – We report on a systematic analysis of the frequency spectrum of a system often considered for quantum computing purposes, metadevice applications, and high-sensitivity sensors, namely a superconducting loop interrupted by Josephson junctions, the core of an rf-SQUID. We analyze both the cases in which a single junction closes the superconducting loop and the one in which the single junction is replaced by a superconducting interferometer. Perturbation analysis is employed to display the variety of the solutions of the system and the implications of the results for the present interest in fundamental and applied research are analyzed.

invited article Copyright © EPLA, 2016

Introduction. – Research on metamaterials and metadevices is receiving much attention from both fundamental science and applications [1,2]. The "functional" features of devices when these are thought to perform specific tasks in response to electromagnetic stimuli, are particularly rich in their required multi-disciplinary understanding. Excellent reviews covering several aspects of the developments of this new topic have already appeared [3,4]. Condensed-matter systems which could operate at specific electromagnetic wavelengths performing particular operations occupy a somewhat privileged role and, within this framework, superconducting systems have already been considered by several groups [5,6].

Josephson junction systems, having the ability to provide active response in a continuum range of wavelengths in the microwave and millimeter wave range of the electromagnetic spectrum, have been considered [7] due to the inherent ac-Josephson relationship, which uniquely relates frequency (ν) to voltage V, namely $h\nu = 2eV$, where h is Planck's constant and e the elementary charge. The ratio $h/2e = \Phi_0 = 2.07 \times 10^{-15}$ Wb is the flux quantum [8].

A superconducting loop interrupted by a Josephson junction, the core of the rf-SQUID [8], is a system combining two fundamental phenomena in superconductivity, namely flux quantization and Josephson effect; these loops have been extensively investigated since the discovery of the Josephson effect [8]. An rf-SQUID core exploits the Josephson sensitivity to the electromagnetic field thereby achieving unprecedented magnetic-flux sensitivities. Today's rf-SQUID relies just on a superconducting ring made by planar thin films interrupted by a tunnel junction, a device which is not beyond the reach of contemporary medium-level technological facilities.

The interest for the rf-SQUID core, relevant in macroscopic quantum tunneling [9], in quantum computation [10] and metamaterial research [6], has often required operation of the system under the application of external microwaves, or pulsed-microwave bursts, and we believe that is relevant for tracing a detailed spectrum of proper modes in the system. Our analysis will be carried out in two steps: in the next section we trace the properties of a superconducting loop interrupted by a single Josephson junction while in the third section we analyze the case in which the single Josephson junction of the loop is replaced by a two-junction interferometer. This system was first investigated by Blackburn and Smith [11] and then taken as a basis for barrier-modulated Josephson macroscopic quantum tunneling devices [12,13]. Metadevice applications based on rf-SQUIDs, and two-dimensional arrays of rf-SQUIDs cores, have been recently reported [14].

[(a)] Also at: CNR-SPIN Institute - Genova, Italy.

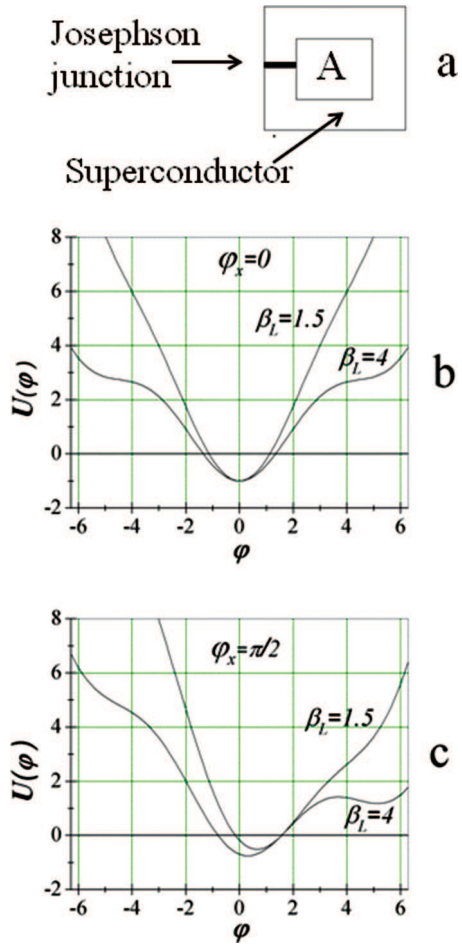

Fig. 1: (a) The system subject of the present work: a superconducting loop closed by a Josephson junction; (b) example of the potential for different values of the normalized inductance of the loop but for zero applied external flux; (c) examples of the potential for an applied external flux $\varphi_x = \pi/2$. It is herein assumed that the direction of the external magnetic field is always orthogonal to the plane of the loop. We can see that the effect of the applied flux is to introduce an asymmetry in the shape of the potential. The curves for the plotted potential are obtained from eq. (4).

A systematic analysis of the frequency spectrum can be relevant within the framework of the selective microwave filters described in the context of these and of the other publications mentioned above.

Single-junction case. – We start from the rf-SQUID (core) equation for the magnetic flux Φ through a superconducting loop interrupted by a Josephson junction shown in fig. 1(a) [8],

$$\frac{\Phi_0 C}{2\pi}\ddot{\Phi}+\frac{\Phi_0}{2\pi R}\dot{\Phi}+I_c \sin\left(2\pi\frac{\Phi}{\Phi_0}\right)+\frac{\Phi_0}{2\pi L}\left(\Phi-\Phi_x\right)=0. \quad (1)$$

In this equation C is the total capacitance of the junction, R a resistance modeling loss due to subgap tunneling, the quantity Φ_x represents an externally applied magnetic flux, and Φ_0 is the flux quantum. In what follows we assume that the external magnetic field has a time-constant direction orthogonal to the plane of the loop. Normalizing time to $(1/\omega_j) = (2\pi I_c/\Phi_0 C)^{1/2}$, the current to the maximum Josephson current I_c, the flux to $\Phi_0/2\pi$, and defining the parameters $\alpha = 1/\sqrt{\beta_c} = (\Phi_0/2\pi I_c R^2 C)^{1/2}$, and $\beta_L = 2\pi L I_c/\Phi_0$, the above equation for the flux through the loop becomes

$$\ddot{\varphi}+\alpha\dot{\varphi}+\sin\varphi+\frac{1}{\beta_L}\left(\varphi-\varphi_x\right)=0, \quad (2)$$

where φ is the phase difference across the junction closing the loop. The static solutions of eq. (2) in the absence of applied external flux are determined by the solutions to the equation

$$\sin\varphi+\frac{\varphi}{\beta_L}=0. \quad (3)$$

Let us call φ_e an equilibrium angle solution of eqs. (2) and (3). We note that these angles correspond to the minima of the rf-SQUID core potential for eq. (2), with the particle sitting at the bottom of the wells. This potential, normalized to the Josephson energy $\Phi_0 I_c/2\pi$, is

$$U\left(\varphi\right)=\frac{1}{2\beta_L}(\varphi-\varphi_x)^2-\cos\varphi. \quad (4)$$

Plots of this potential are shown in fig. 1(b), (c). We now look for solutions of eq. (2) (no loss, $\alpha = 0$, and no applied magnetic flux $\varphi_x = 0$) of the type

$$\varphi=\varphi_e+\psi, \quad \text{with } \psi \ll 1. \quad (5)$$

It is worth recalling that in typical experiments $\alpha \approx 10^{-4}$ [10–13] which makes the omission of dissipation in our considerations a good approximation. Later we will comment more quantitatively on this assumption, showing that the influence of such small loss terms is really not relevant for the frequency spectrum. The condition (5), to the first order in ψ, gives $\sin\varphi = \sin\varphi_e + \psi\cos\varphi_e$, and transforms eq. (2) to the following equation for ψ:

$$\ddot{\psi}+\left(\cos\varphi_e+\frac{1}{\beta_L}\right)\psi+\left[\left(\frac{\varphi_e}{\beta_L}\right)+\sin\varphi_e\right]=0. \quad (6)$$

The term in the square brackets is eq. (3) and vanishes since φ_e is a solution of eq. (3), and so eq. (6) becomes

$$\ddot{\psi}+\left(\cos\varphi_e+\frac{1}{\beta_L}\right)\psi=0, \quad (7)$$

which is the harmonic-oscillator equation for the variable ψ. Defining $\xi = (\cos\varphi_e + \frac{1}{\beta_L})$ this equation has modes with frequency $\Omega = \xi^{1/2}$ meaning that the "proper" oscillation frequency of the system in unnormalized units is

$$\omega_0=\omega_j\Omega=\omega_j\xi^{1/2}=\omega_j\left(\cos\varphi_e+\frac{1}{\beta_L}\right)^{1/2}. \quad (8)$$

This equation shows the effect of β_L on the proper oscillation frequencies. Taking the limits $\beta_L \to \infty$ or $\beta_L \to 0$

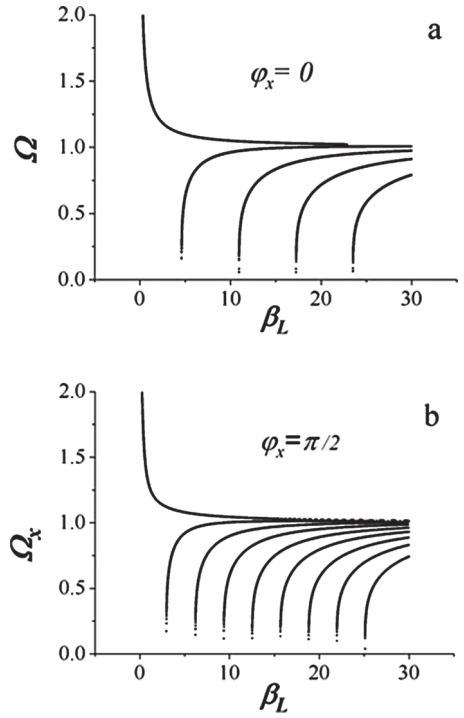

Fig. 2: Dependences of the oscillation frequencies, around the equilibrium angle, on the normalized loop inductance β_L for zero applied external magnetic flux (a) and for a normalized flux $\varphi_x = \pi/2$ (b).

in eq. (3) we see that the resulting allowed static solutions are, respectively, $\varphi_e = 2k\pi$, k integer, and $\varphi_e = 0$. The corresponding resonant frequencies are, respectively, the usual zero-bias Josephson plasma frequency (for all k integers) and $\omega_0 \to \infty$.

Figure 2(a) shows the frequency dependence on β_L around the stable equilibrium points. The plot is obtained for zero applied external magnetic flux and we can see that multiple frequencies are allowed for increasing β_L. This plot has been obtained by sweeping the value of the normalized flux in the interval $[-8\pi, 8\pi]$ while finding numerically the minima of the potential (eq. (4)) for each given value β_L. The mode whose frequency tends to infinity for $\beta_L \to 0$ is the one of the center well of the potential while the others are those that develop for increasing values of β_L in the side wells.

Let us now turn to the non-zero applied flux case for which we apply the same analysis performed for eq. (2). That approach can be readily be applied to the non-zero flux case which will lead to the two equations

$$\sin\varphi + \frac{1}{\beta_L}(\varphi - \varphi_{ex}) = 0 \tag{9}$$

for the equilibrium angles and

$$(\Omega_x)^2 = \left(\cos\varphi_{ex} + \frac{1}{\beta_L}\right) \tag{10}$$

for the system frequencies. Note that Ω_x becomes the previous Ω for the unbiased case, when $\varphi_x = 0$. The unnormalized angular frequency ω_x corresponding to each Ω_x value will be

$$\omega_x = \omega_j \sqrt{\cos\varphi_{ex} + \frac{1}{\beta_L}}. \tag{11}$$

Although eq. (11) looks formally identical to eq. (8) the external flux here introduces an asymmetry in the potential and the minima leading to values of φ_{ex} (eq. (9)) that are different from those of eq. (3). In fig. 2 we can see the branching of the curves of fig. 2(b) obtained for an applied external flux equal to a quarter of the flux quantum (which is 2π in normalized units). The plots of fig. 2 were obtained by sweeping values of the phase in the interval $[-8\pi, 8\pi]$. To each of the frequency branches shown in the figures naturally corresponds a specific minimum of the potential.

The spectrum of the possible frequencies as a function of the externally applied flux can be obtained from eq. (10) employing the φ_{ex} solutions of eq. (9) which we find numerically. In fig. 3 we see how, in the opposite plots the $\beta_L = 1$ singled-value spectrum evolves in a crossing-branches spectrum for increasing values of β_L. For $\beta_L = 2$ (fig. 2(b)) and $\beta_L = 4$ the resonance curves only cross at multiples of half the flux quantum (π in our normalized units) while already for $\beta_L = 6$ the crossings of the branches take place for half integer values of the flux quantum. The plots of fig. 3 have been obtained by sweeping the φ values in the range $[-4\pi, 4\pi]$. The resonant branches represent oscillation frequencies in different wells of the rf-SQUID potential.

More crossings for increasing values of β_L take place generating complex patterns. An example is given in fig. 4 for $\beta_L = 10$ (a) and $\beta_L = 20$ (b). We display here the results only in the field interval $[0, 2\pi]$ and, moreover in fig. 4(b) only a narrow segment of the plot along the vertical direction is presented in order to preserve clarity. At this point ($\beta_L = 20$) we see that three crossings take place at half the flux quantum, meaning, for example, that possible operation of the device when biased with a dc magnetic flux linking half a magnetic flux through the loop is likely going to be difficult to control in terms of frequency response. In fig. 2(b)–(d) we have only two resonant branches close to the $\varphi_x = \pi$ point, whereas in fig. 4(a) and (b) we have, respectively, four and six resonance branches: To these resonant branches naturally one can associate different classical energy levels corresponding to given values of the external flux.

We would like to emphasize that operation of the rf-SQUID core has often been considered by biasing the system with an external flux which would generate half of the flux quantum in the rf-SQUID core [9,12,13]. In this case we can see in fig. 3 and fig. 4 that the crossing of branches corresponding to different frequencies is remarkable and the resulting dynamics could be noticeably complex. For $\beta_L = 10$ we have two frequency crossings for $\varphi_x = \pi$ separated roughly by a (normalized) frequency

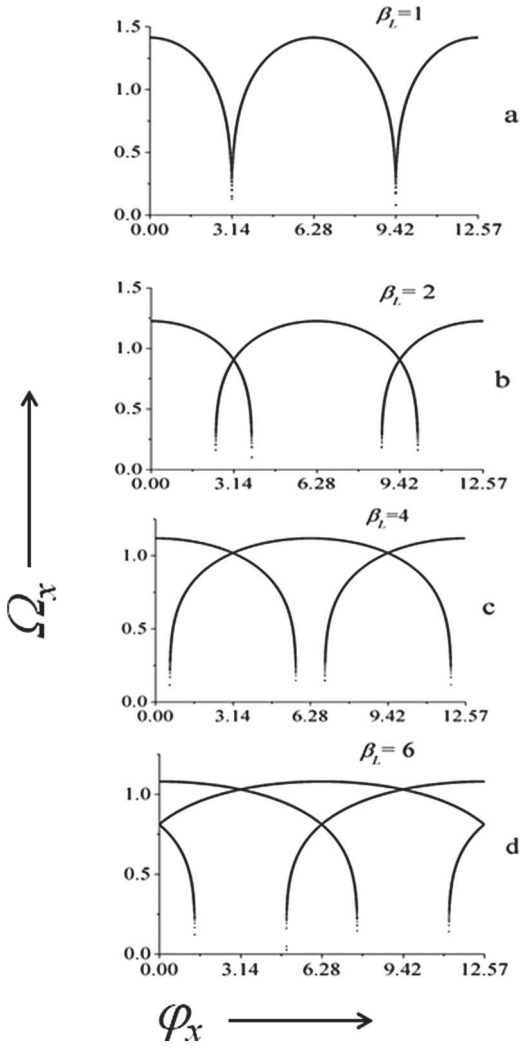

Fig. 3: The frequency spectrum of the rf-SQUID core as a function of an applied flux for different values of the normalized inductance β_L, indicated in the panels. We can clearly see that, for increasing values of this parameter, the system develops a number of crossing states of the resonance curves. All the crossings occur for integer and half-integer values of the flux quantum (2π in our normalized units).

gap of 0.2, while for $\beta_L = 20$ we have three crossings separated by tenths normalized frequency units. Naturally, the closer we get to integers and half-integers values of the flux quantum the smaller is the difference in frequency (and energy) between the different states corresponding to different branches. Overall we can say that the system behaves as a metaatom [6,14] with different energy states available in correspondence to given values of the applied field. These frequencies naturally represent oscillation frequencies in the wells of the potential (4).

The effect of dissipation on eq. (4) can be readily evaluated using the ansatz (5) for eq. (2). In this case we get

$$\ddot{\psi} + \alpha\dot{\psi} + \left(\cos\varphi_{ex} + \frac{1}{\beta_L}\right)\psi = 0, \qquad (12)$$

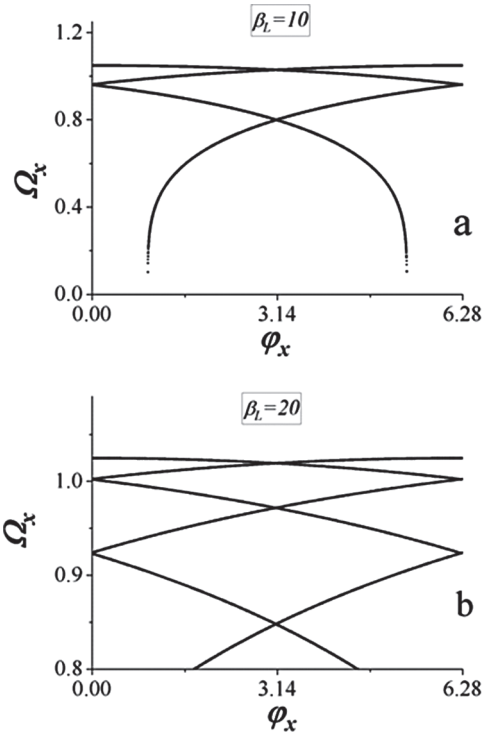

Fig. 4: Two more examples of (φ_x, Ω_x) plots exhibiting the more complex structures that develop for increasing values of the normalized inductance of the rf-SQUID loop. In this figure, as in the others, the phase of the potential is swept in the interval $[-4\pi, 4\pi]$.

which tells us that, in the presence of dissipation, the angular frequency of underdamped oscillations will be

$$(\Omega_\alpha)^2 = (\Omega_x)^2 - \alpha^2/4 \quad \text{or} \quad \Omega_\alpha = [(\Omega_x)^2 - \alpha^2/4]^{1/2}. \qquad (13)$$

From which we see that corrections, given the values of α in the experiments [10–13] typically of the order of 10^{-4} and below, should not be really significant.

Double-junction rf-SQUID. – We now consider the two-junctions rf-SQUID system shown in fig. 5(a). Our starting point for the analysis are eqs. (7) and (8) of ref. [11]. Normalizing in these equations time and currents as we did for eq. (1) we obtain the two coupled differential equations:

$$\ddot{\varphi}_a + \alpha\dot{\varphi}_a + \cos\varphi_b \sin\varphi_a + \frac{1}{2\beta_{ab}}(\varphi_b - \varphi_x) = 0, \qquad (14)$$

$$\ddot{\varphi}_b + \alpha\dot{\varphi}_b + \cos\varphi_a \sin\varphi_b + \frac{1}{2\beta_b}(\varphi_b - \lambda\varphi_x) = 0. \qquad (15)$$

The subscripts a and b for the normalized fluxes refer to the large area loop (a) and small area loop (b), and the two parameters $\beta_{ab} = 2\pi I_c\,(L_a + L_b)/\Phi_0 = \beta_a + \beta_b$ and $\beta_b = 2\pi I_c L_b/\Phi_0$ are the normalized inductances corresponding, respectively, to the sum of the areas of the two loops and to the area of the single smaller loop; β_a is the normalized inductance of a loop having area A. The factor φ_x accounts

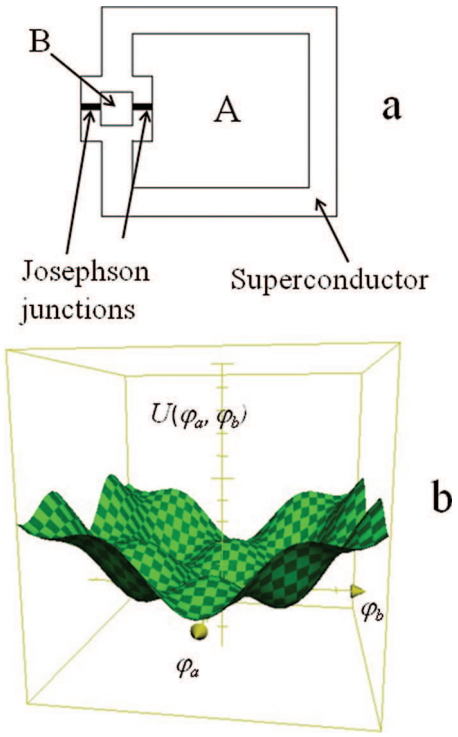

Fig. 5: (a) The "double"-loop rf-SQUID system and its potential (b). The analytical form of the potential is written in eq. (22). A and B represent the areas of the two superconductive loops. Here φ_a and φ_b are spanned between -2π and 2π, while the potential is spanned between -3 and 10.

for an external magnetic flux applied uniformly over the two loops and $\lambda = [1+2(A/B)]^{-1} = 1/[(2\frac{\beta_{ab}}{\beta_b})-1]$ is a geometrical factor since A and B are, respectively, the areas of the big loop and of the small loop in fig. 5(a) [11]. In terms of the Josephson phase differences shown in fig. 1(b) φ_1 and φ_2 we have $\varphi_1 = \varphi_a + \varphi_b$ and $\varphi_2 = \varphi_a - \varphi_b$.

We look, similarly to what we did in the previous section, for solutions of eqs. (14) and (15) in the forms

$$\varphi_a = \varphi_{ea} + \psi_a \quad \text{with} \quad \psi_a \ll 1, \tag{16}$$
$$\varphi_b = \varphi_{eb} + \psi_b \quad \text{with} \quad \psi_b \ll 1. \tag{17}$$

In these equations φ_{ea} and φ_{eb} are the equilibrium angles corresponding to solutions of (14) and (15) in the static limit. We are interested again in solutions of eqs. (14) and (15) in the form of small oscillations around equilibrium angles φ_{ea} and φ_{eb}. Inserting eqs. (15) and (16) into eqs. (13) and (14), and using the small amplitudes oscillation limits $\sin\varphi_a = \sin(\varphi_{ea}+\psi_a) = \sin\varphi_{ea} + \psi_a\cos\varphi_{ea}$ and $\sin\varphi_b = \sin(\varphi_{eb}+\psi_b) = \sin\varphi_{eb} + \psi_b\cos\varphi_{eb}$, we obtain the two coupled equations

$$\ddot{\psi}_a + \alpha\dot{\psi}_a + \left(\cos\varphi_b\cos\varphi_{ea} + \frac{1}{2\beta_{ab}}\right)\psi_a = 0, \tag{18}$$
$$\ddot{\psi}_b + \alpha\dot{\psi}_b + \left(\cos\varphi_{eb}\cos\varphi_a + \frac{1}{2\beta_b}\right)\psi_b = 0. \tag{19}$$

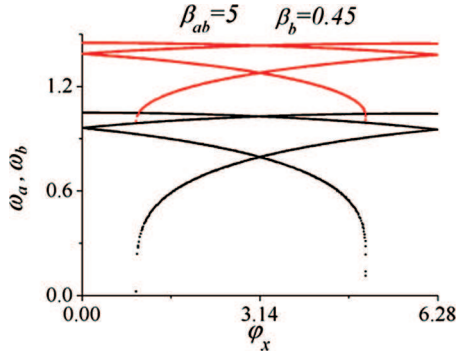

Fig. 6: The two frequency bands obtained when the inner loop area B is ten times smaller than the area A. In order to calculate the minima of the potential the phases φ_a and φ_b are swept in the interval $[-4\pi, 4\pi]$.

The two equations above are coupled damped harmonic-oscillator equations. Neglecting the loss term (an assumption which can be justified just as we did above for the single-junction case) the proper frequencies associated with eqs. (18) and (19) are

$$\omega_a = \sqrt{\cos\varphi_b\cos\varphi_{ea} + \frac{1}{2\beta_{ab}}} \tag{20}$$

and

$$\omega_b = \sqrt{\cos\varphi_{eb}\cos\varphi_a + \frac{1}{2\beta_b}}. \tag{21}$$

When looking for stable equilibrium points of the coupled system (14), (15) and (18), (19), both the conditions for the equilibrium on the two phases must be fulfilled and, therefore, in eqs. (20) and (21) the cross-cosine terms just become $\cos\varphi_{eb}\cos\varphi_{ea}$ in both equations. It is worth noting that the static solutions of the system of equations (1), (2) also correspond to the minima of the potential of our physical system. This potential, normalized to the Josephson energy $\Phi_0 I_c/2\pi$, reads

$$U = \frac{(\varphi_x-\varphi_a)^2}{4\beta_{ab}} + \frac{(\lambda\varphi_x-\varphi_b)^2}{4\beta_b} - \cos\varphi_a\cos\varphi_b. \tag{22}$$

This two-dimensional potential is plotted in fig. 5(b) for two $\beta_{ab} = 6$ and $\beta_b = 3$. Note that this corresponds to the case in which the areas A and B of the two loops are equal: This is not a condition that we will further investigate (we will work in the approximation $\beta_{ab} \gg \beta_b$) but we have chosen these parameters in order to illustrate the nature of the potential and its characteristic features. It can be readily seen that setting to zero the first derivatives of the potential (22) corresponds to the static solutions of eqs. (14) and (15). We are here interested in investigating the frequency spectrum dependence of our system upon the externally applied magnetic flux φ_x. In order to do so we will first find, numerically, the minima of the potential function (22). These minima will provide the values of

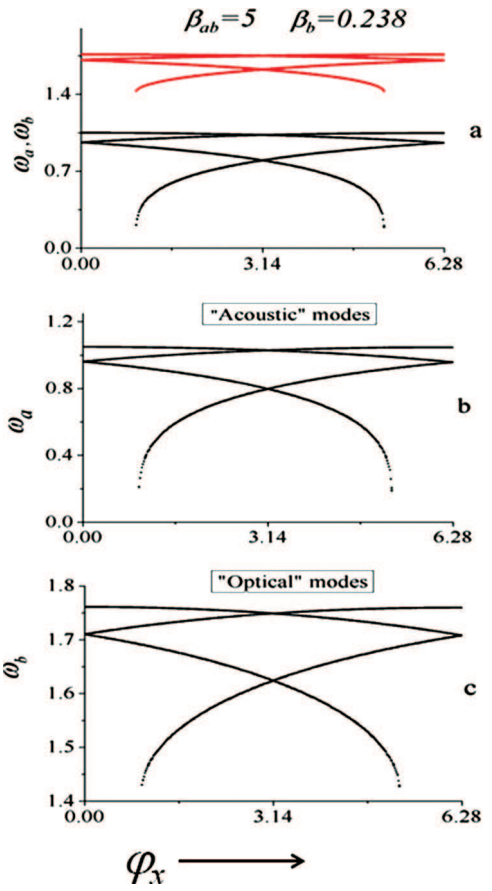

Fig. 7: (a) The frequency "spectrum" of the double squid as a function of the externally applied flux when $A = 20B$. The expansion of the two frequency bands is shown in (b) and (c). Here we can see the analogous shapes of the bands.

the phase to be substituted in eq. (20) and eq. (21) for determining the values of the frequencies.

In order to find the minima of the potential (22) we swept both the phases φ_a and φ_b in the interval $[-4\pi, 4\pi]$ and the externally applied flux between 0 and 2π. Setting $\beta_{ab} = 5$ and choosing a very small value for the parameter β_b (10^{-5}) we found, as expected, since the presence of the second loop is negligible, a "flux spectrum" identical to that of a single-junction rf-SQUID core having a value of the normalized inductance $\beta_L = 10$ (see fig. 4(a)). This is correct since the critical current of our system is twice that of a single-junction rf-SQUID. We have then changed the values of the normalized inductances of the two loops trying to maintain our calculations close to realistic experimental parameters [12,13]. In fig. 6 we see the "flux spectrum" obtained for $\beta_{ab} = 5$ and $\beta_b = 0.45$ corresponding to having the area (B) of the smaller loop in fig. 5(a) ten times smaller than the area (A) of the larger loop. We can here see that there are now two bands of frequencies and the maximum of the upper band is 1.44 as expected from eq. (21). The upper band is just a replica, at higher frequencies, of the pattern exhibited for lower frequencies. In fig. 7(a) we show the spectrum obtained by setting $\beta_{ab} = 5$ and $\beta_b = 0.238$, corresponding to the

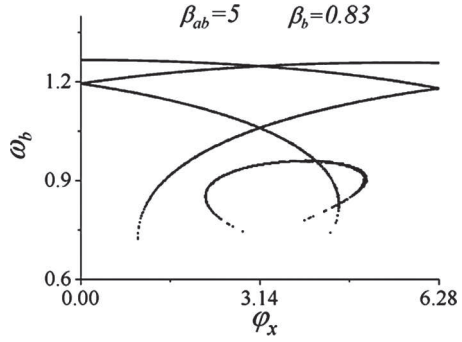

Fig. 8: An example of the somewhat irregular "branches" appearing in an optical band when the normalized inductance of the inner loop gets close to 1. In this case $A = 5B$.

case in which the area B is 20 times smaller than A. We can clearly see that the "optical" mode moves up while the "acoustic" mode remains in the same position as in fig. 6(b). In fig. 7(b), (c) we show details of the frequency bands demonstrating that, apart from occupying a more compressed frequency interval, the two "bands" have analogous shape and branch crossing.

We have found the patterns of figs. 6 and 7 to be very controllable features of the spectrum of the two-junctions rf-SQUID system. This is naturally a very interesting phenomenon to consider in perspective of metadevice applications. Beside the tuning of the modes of the systems as a function of the external flux we find that an adequate choice of the ratios between the areas of the loops generates an additional (higher) band of frequency in which the system can operate. However, we have also found that attention must be paid to not letting the normalized inductance of the inner loop be close to 1. In this case we reach the point in which the single junctions of the loop could generate crossings of the modes and the resulting features become very irregular and, most likely, very difficult to control. An example of this phenomenon is shown in fig. 8 for which we have chosen $\beta_{ab} = 5$ and $\beta_b = 0.83$: we can see that an additional, somewhat irregular, branch appears in the frequency-*vs.*-flux pattern of the "optical" modes. The "acoustic" modes in this case showed the same type of pattern at lower frequencies.

We point out that several experiments have been performed independently controlling the fluxes applied to the two loops of the "double SQUID" [12,13]. Having the possibility to tune independently the fluxes means that one could perform a selection between the "acoustic" and "optical" band of operation.

Conclusions. – The analysis, performed in a perturbation approach for finding the oscillation modes of rf-SQUID cores around the equilibrium angle, has shown, a variety of configurations and crossings of the branches of the different modes. The crossings of the branches occur when the external magnetic flux attains half and integer multiple values of the flux quantum. Close to these values of the external flux the response of the system to

an external microwave/millimeter-wave excitation could have intriguing aspects; it is worth noting that this specific magnetic-flux bias has been often chosen for macroscopic quantum tunneling and coherence investigations [9,12]. The analysis of the case in which the junction closing the rf-SQUID loop is replaced by a double-junction interferometer has shown additional features of the system corresponding to a splitting of the response of the modes of the system in a lower ("acoustic") and a higher ("optical") frequency band. The degeneracy can be governed by adequately choosing the areas (and the inductances) of the two loops of the device. Potential applications such as those described in ref. [14] or the wide spectrum described within metamaterial research [6] open interesting perpectives for the future of a system which has already substantially contributed to the development of the research in fundamental and applied superconductivity.

As far as microwave and millimeter-wave fields reaching the rf-SQUID region are concerned, one can reasonably assume that the radiation fields will be distributed uniformly in the loop areas and in the junctions; however, we should bear in mind that the magnetic fields in the two loops of the double-loop rf-SQUID can be controlled independently [12,13]. This means that the two modes, the acoustic mode and the optical one, can be tuned independently and this represents another interesting direction for future devices. From the "rf" point of view, however, the relevant feature of the system having two frequency bands remains unchanged. High-frequency features of the Josephson junctions have demonstrated, over the years, that this field is very rich and intriguing and there still are features which have not been explained [15]. We have herein provided evidence, through a systematic analysis, that a basic superconducting system could lead to further experimental rf work and devices.

Throughout the paper we have normalized time to the inverse of zero-bias Josephson plasma angular frequency ω_j. This is a very well-known parameter in Josephson research and, for current densities in the range (100–1 kA) A/cm^2 it attains values in the interval $(0.4\text{–}1.3)\times 10^{12}$ rad/s meaning that the frequencies will be roughly in the range 60–200 GHz. Here we have considered a standard trilayer Nb-NbAlOx-Nb fabrication process for which the specific capacitance of the junctions is of the order of 0.05 F/m^2 [15]. From these estimates it follows that we investigated issues in a range of the electromagnetic spectrum which is still of noticeable interest for applications. An "optical" mode of the double rf-SQUID that we analyzed could have proper frequencies around 300 GHz.

REFERENCES

[1] Zheludev N. I. and Kivshar Y. S., *Nat. Mater.*, **11** (2012) 917.

[2] Kats M. A. *et al.*, *Phys. Rev. X*, **3** (2013) 041004.

[3] Walia S. *et al.*, *Appl. Phys. Rev.*, **2** (2015) 011303.

[4] Liu Yongmin and Zhang Xiang, *Chem. Soc. Rev.*, **40** (2011) 2494.

[5] Chen H.-T. *et al.*, *Phys. Rev. Lett.*, **105** (2010) 247402; Kurter C. *et al.*, *Phys. Rev. Lett.*, **107** (2011) 043901; Ghamsari B. G., Abrahams J., Remillard J. and Anlage S. M., *Appl. Phys. Lett.*, **102** (2013) 013503.

[6] Jung P., Ustinov A. V. and Anlage S. M., *Supercond. Sci. Technol.*, **27** (2014) 073001.

[7] Castellanos-Beltran M. A. *et al.*, *Nat. Phys.*, **4** (2008) 928; Jung P. *et al.*, *Appl. Phys. Lett.*, **102** (2013) 062601.

[8] Barone A. and Paternò G., *Physics and Applications of The Josephson Effect*, (J. Wiley, New York) 1982, Chapt. 12 (particularly sect. 12.2 and eq. (12.2.15)), and Chapt. 13; Van Duzer T. and Turner C. W., *Principles of Superconducting Devices and Circuits* (Elsevier, North-Holland, New York) 1981, sect. 5.11, eq. (3); Clarke J. and Braginsky A. I. (Editors), *The SQUID Handbook*, Vol. **I**, *Fundamentals and Technology of SQUIDs and SQUID Systems* (Wiley-VCH Verlag GmbH & Co. KGaA, Weinheim) 2004.

[9] Kurkijärvi J., *Phys. Rev. B*, **6** (1972) 832; Cosmelli C. *et al.*, *Phys. Rev. Lett.*, **82** (1999) 5357; Ovchinnikov Yu. N. *et al.*, *Phys. Rev. B*, **71** (2005) 024529; Blackburn J. A., Cirillo M. and Grønbech-Jensen N., *Phys. Rep.*, **611** (2016) 1.

[10] Steffen M. *et al.*, *Science*, **313** (2006) 1423; Sillanpää M. A. *et al.*, *Nature*, **449** (2007) 438; Grønbech-Jensen N., Marchese J. E., Cirillo M. and Blackburn J. A., *Phys. Rev. Lett.*, **105** (2010) 010501.

[11] Blackburn J. A. and Smith H. J. T., *J. Appl. Phys.*, **48** (1977) 2961.

[12] Han S., Lapointe J. and Lukens J. E., *Phys. Rev. B*, **46** (1992) 6338; Rouse R., Han S. and Lukens J. E., *Phys. Rev. Lett.*, **75** (1995) 1614; Friedman J. R. *et al.*, *Nature*, **406** (2000) 43.

[13] Castellano M. G. *et al.*, *Phys. Rev. Lett.*, **98** (2007) 177002.

[14] Caputo J.-G., Gabitov I. and Maimistov A. I., *Phys. Rev. B*, **85** (2012) 205446; **91** (2015) 115430.

[15] Lucci M., Badoni D., Merlo V., Ottaviani I., Salina G., Cirillo M., Ustinov A. V. and Winkler D., *Phys. Rev. Lett.*, **115** (2015) 107002; Cirillo M., Modena I., Santucci F., Carelli P. and Leoni R., *Phys. Lett. A*, **167** (1992) 175; Grønbech-Jensen N. and Cirillo M., *Phys. Rev. B*, **50** (1994) 12851.